LONGITUDINAL SPACE CHARGE EFFECTS IN THE JLAB IR FEL SRF LINAC

C. Hernandez-Garcia*, K. Beard, C. Behre, S. Benson, G. Biallas, J. Boyce, D. Douglas, H. F. Dylla, R. Evans, A. Grippo, J. Gubeli, D. Hardy, K. Jordan, L. Merminga, G. Neil, J. Preble, M. Shinn, T. Siggins, R. Walker, G. P. Williams, B. Yunn, S. Zhang, TJNAF, Newport News, VA 23606, USA

Abstract

Observations of energy spread asymmetry when operating the Linac on either side of crest and longitudinal emittance growth have been confirmed by extending PARMELA simulations from the injector to the end of the first SRF Linac module. The asymmetry can be explained by the interaction of the accelerating electric field with that from longitudinal space charge effects within the electron bunch. This can be a major limitation to performance in FEL accelerators.

INTRODUCTION

During the commissioning of the Jefferson Lab 10 kW Upgrade IR FEL several intriguing questions regarding the performance of the injector and the longitudinal phase space management were encountered. The full-energy momentum spread of the beam showed an asymmetry as a function of linac gang phase. Furthermore, the compressed bunch length at the wiggler and therefore the longitudinal emittance showed a clear dependence on transverse match into and through the linac and was as much as a factor of 4 larger than the emittance predicted at the end of the injector. Operational and performance issues in the linac such as cavities being out of phase and/or wake fields were ruled out as the source of the problem after careful investigation. Then, PARMELA modeling was extended from injection to the end of the first cryo-module to study the longitudinal beam dynamics as a function of linac gang phase [1].

The machine design for the Jefferson Lab 10 kW Upgrade IR FEL has been described in detail elsewhere [2]. It consists of a 10 MeV injector, a linac comprised of three Jefferson Lab cryo-modules, and a recirculation lattice. The machine layout is shown in Figure 1.

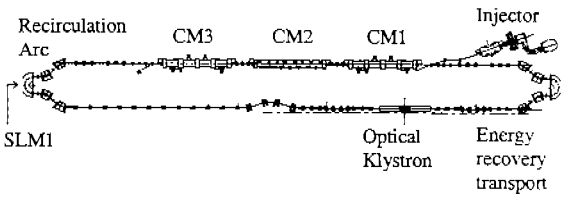

Figure 1: Jefferson Lab 10 kW Upgrade IR FEL. CM1, CM2, and CM3 are CEBAF-type cryo-modules. SLM1 is a synchrotron light monitor.

* Corresponding author: Tel: 1-757-269-6862; fax:1-757-269-5519; E-mail address: chgarcia@jlab.org

The injector consists of a high-voltage-DC GaAs photocathode gun driven by a frequency-doubled Nd:YLF laser, a 10 MeV quarter cryo-unit with two 5-cell CEBAF cavities, a transverse match section and a bunch compressor [3]. The photocathode gun delivers 135 pC, 23 ps rms-long electron bunches operating at 350 kV in pulse (demonstrated up to 8 mA) and CW (demonstrated up to 9.1 mA) modes [4]. The photocathode gun performance has been studied earlier [5]. After initial acceleration at 10 MeV, the electron beam is transversely matched to the linac by means of a quadrupole telescope, longitudinal match is provided by an achromatic compressor chicane [6].

The linac further accelerates the electron beam at energies between 80 and 200 MeV. The first (CM1, see Figure 1) and third (CM3) cryo-modules are conventional 5-cell CEBAF cavities, while the middle module (CM2) is based on a new 7-cell JLab design [7]. The beam is accelerated off-crest to impose a phase correlation on the longitudinal phase space.

The first part of the recirculator transports the beam after acceleration to the FEL. A six quad telescope transversely matches the high-energy beam to a 180°-recirculator arc, which is based on a Bates geometry [8]. At the middle of the arc, a synchrotron light monitor (SLM1, see Figure 1) is employed to measure the energy spread after acceleration. The beta function is always very small at this location so the spot size is dominated by the energy spread. After interaction with the FEL, the beam is re-circulated for energy recovery by a second Bates-style arc.

MEASUREMENTS AND MODELING

With only the first and third cryo-modules installed in the machine at the time (CM1 and CM3), an asymmetry in the beam momentum spread as a function of linac gang phase was observed during the FEL commissioning activities. The injector had been setup accordingly to PARMELA to produce an upright longitudinal phase space distribution at the entrance of the linac [4], as shown in Figure 2.

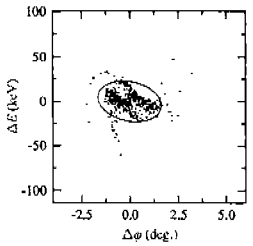

Figure 2: PARMELA longitudinal distribution at the entrance of the first cryo-module. The predicted full energy spread is 44.3 keV, the full bunch length is 6 ps (or 11.1°), and the longitudinal emittance is 16.8 ps-keV

If the distribution is upright at injection, then the beam momentum spread after acceleration (measured at SLM1 in Figure 1) should be symmetric around crest. This was not the case. With the injector se up to produce the phase space in figure 2, the beam full momentum spread when accelerating 15° ahead of crest (nominal operating conditions for a longitudinal match to the wiggler) was 1%, and 1.5% when accelerating 15° behind crest, was 1.5%. The full-energy momentum spread is established from a spot size measurement at a point of high dispersion by

$$\frac{\Delta E_W}{E_W} = \frac{\Delta x}{\eta_x}, \qquad (1)$$

where ΔE_W is the beam full-energy spread, E_W is the beam energy at the high dispersion point (SLM1 at the middle of the first recirculator arc, see Figure 1), Δx is the spot size and η_x is the dispersion function of the arc dipole (70 cm). The calibration was performed by measuring the displacement of the centroid of the spot in the SLM1 video screen when the beam energy was changed by 1%. Figure 3a shows a snapshot of the synchrotron light at SLM1. The spot size is measured by means of a frame grabber software that gives the spot size profile in pixels for both x and y-axis [9]. Figure 3b shows the frame grabber output generated from the spot shown in Figure 3a.

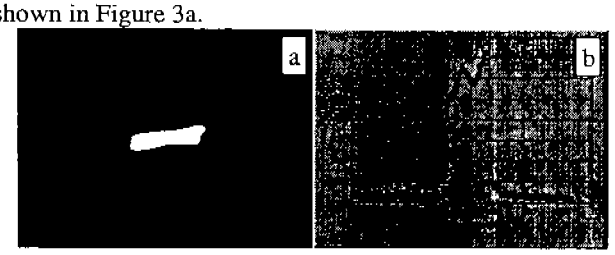

Figure 3: (a) Snapshot of the synchrotron light monitor in the middle of the first recirculation arc. (b) Output generated by the frame grabber to measure the spot size of the synchrotron light shown in (a).

Assuming that the asymmetry in the energy spread is a linear effect (this assumption was later confirmed by PARMELA simulations), the injected bunch full length (in ps) can be established by back-propagating the average of energy spreads at either side of crest via the following

$$\Delta t = \frac{\Delta E_W}{E_W} \frac{\left(1 + E_I / E_L\right)}{\omega \tan \phi}, \qquad (2)$$

where $\Delta E_W / E_W$ is the full energy spread at the wiggler, E_I is the injector energy, E_L is the energy gain in the linac, ω is the accelerator frequency, and ϕ is off-crest phase. With the downstream cavity in the injector operating at 20° off crest and the linac at 15° off crest, the measured average of the energy spread is 0.0125. For E_W = 80 MeV, and E_{inj} =9.2 MeV, equation 2 yields Δt = 5.6 ps. This result agrees quite well with PARMELA (see Figure 2).

The performance of the injector regarding longitudinal phase space management was questioned after eliminating operational and performance issues in the linac as a source of the problem (i.e. one or more cavities being out of phase, wake fields, etc.). PARMELA modeling was then extended from the injector to the end of the first cryo-module. The electron beam energy at injection is 9.2 MeV, therefore no transverse space charge effects are expected from PARMELA through the cryo-module.

However, PARMELA indicates that longitudinal space charge will induce what appears to be a phase-dependent asymmetry in the beam momentum spread during and after acceleration. When accelerating 15° ahead of crest the model predicts an increase in the rms energy spread from 45.3 keV at the entrance of the first cryo-module to 520 keV at the exit. For acceleration behind crest the predicted full energy spread is 659 keV at the exit of the cryo-module. These results are shown in figure 4.

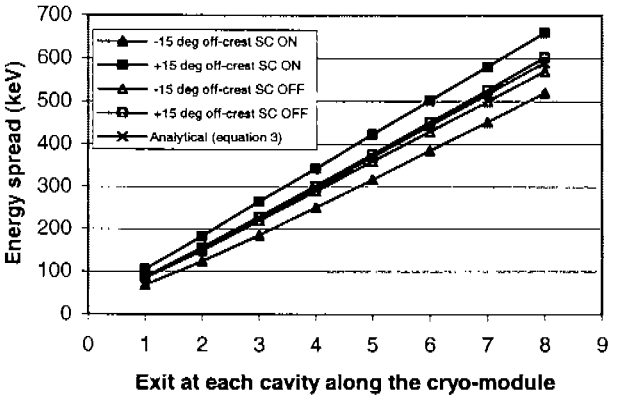

Figure 4: PARMELA calculations at either side of crest show the growth in the imposed correlated energy spread (Space Charge ON). The correlated energy spread (SC OFF) grows as well and is in close agreement with equation 3 (which has been multiplied by 4).

The predicted asymmetry is on the order of 27% after the first cryo-module alone (which is as far as the

simulation has progressed so far). This result is quite consistent with observed momentum spread asymmetry (50%) at the end of the two cryo-modules (exit of CM3, see Figure 1).

The imposed energy spread (by the RF system during acceleration, without space charge) should be symmetric around crest after acceleration, as expressed by

$$\sigma_E = \sqrt{\sigma_{Einj}^2 + \left(V_{linac}\sin(\phi)\sigma_t\right)^2}\,, \qquad (3)$$

where σ_{Einj} is the injected rms energy spread, V_{linac} is the total accelerating voltage in the linac to that point, ϕ is the off-crest phase, and σ_t is the injected rms bunch length in radians. PARMELA is in good agreement with the Equation 3 when the simulation is carried out with the space charge option turned off, as shown in Figure 4.

ANALYSIS

The longitudinal space charge force within the electron bunch accelerates the head and decelerates the tail, creating a tilt in the longitudinal phase space: the head goes to higher energy, and the tail to lower as the beam travels down the linac. This is the correlated energy spread of the beam due to space charge. When accelerating *ahead* of crest (nominal operating conditions for longitudinal phase space management), the head of the bunch is driven to lower, and the tail to higher energy by the RF field. This imposed phase/energy correlation adds to the correlated energy spread, and the observed momentum spread is *reduced*. On the other hand, acceleration *behind* crest drives the head of the bunch to higher energy, and the tail to lower. The imposed phase/energy then adds to the correlated energy spread and the final energy spread is *increased*. Figure 5 illustrates this mechanism.

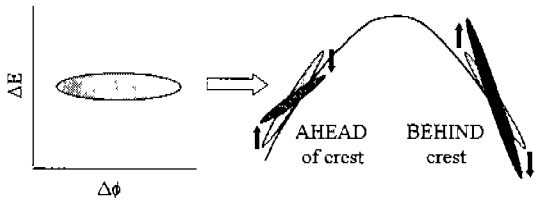

Figure 5: In acceleration ahead of crest, the final momentum spread is reduced. In acceleration behind crest, the final momentum spread is increased.

PARMELA also shows that the longitudinal emittance grows by 57% at the end of the first cryo-module alone. Since the length of the cryo-module is 1/6 of the distance to the wiggler, the longitudinal emittance at the wiggler is around 3 times larger that the longitudinal emittance at injection.

If the injected bunch length is increased, the longitudinal space charge forces are reduced, the energy spread asymmetry alleviated and the longitudinal emittance growth less severe. For a fixed bunch charge, the imposed correlated energy spread depends on the inverse square of the bunch length [10], while the imposed energy spread from the RF system depends linearly on the bunch length (see Equation 3). The optimum bunch length to minimize the correlated energy spread while maintaining the imposed energy spread acceptable for the FEL is about 1.5 times the bunch length with the original injector configuration (1.5 ps rms) [10].

PARMELA predicts that the injected rms bunch length increases from 1.5 ps to 2.37 ps if the downstream cavity in the injector is operated closer to crest (10°, instead of the design value at 20° ahead of crest). The predicted full energy spread at injection decreases from 44.3 keV to 40.5 keV, but the longitudinal emittance increases from 16.8 ps-keV to 19.6 ps-keV. Also, the longitudinal phase space distribution is no longer upright at the entrance to the linac.

The phase/energy slew imposed to the longitudinal distribution by the RF system and space charge effects can be cancelled out with proper longitudinal phase space management elements in the transport system, but the compressed bunch length at the wiggler is limited by the intrinsic longitudinal emittance of the beam due to thermal effects during its creation. The intrinsic longitudinal emittance growth along the cryo-module can be calculated by removing from the bunch particle distribution the quadratic term and the phase/energy slew imposed by the RF. The bunch particle distribution is written by PARMELA at specified intervals along the cryo-module to a separate log file. In another program, each bunch is read back in from the log file, has its longitudinal momentum vs. position fit to a in 2nd order polynomial, then that dependence removed from the distribution and the energy spread recalculated based on the corrected distribution.

Figure 5 shows that the intrinsic energy spread through the cryo-module grows by 76% with for a 1.5 ps rms injected bunch, while for a 2.5 ps rms bunch the intrinsic energy spread increases by 64% at the exit of the cryo-module.

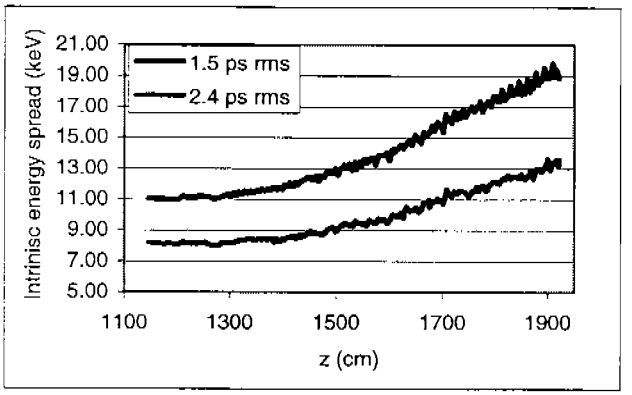

Figure 5: PARMELA-based calculations of the intrinsic energy spread growth along the first cryo-module operating at 15° ahead of crest for two different injected bunch lengths.

The calculations confirm that with a longer injected bunch the longitudinal space charge forces are less severe and the intrinsic energy spread is not only smaller, but it grows slower. Figure 5 also shows that the longitudinal emittance is slightly larger for the longer injected bunch, but grows slower.

When this was implemented, it was quickly confirmed that the asymmetry in the energy spread after acceleration was reduced from 50% to less than 20%. PARMELA shows a reduction in the energy spread asymmetry from 30% to 17%. In fact, with the longitudinal space charge effects less severe with longer bunch at injection, the compressed bunch length at the wiggler was reduced from about 0.8 ps FWHM (injector at 20°, linac at 15° off crest) to less than 0.5 ps FWHM. Laser gain with this configuration was about as strong as the previous configuration but peak efficiency in the detuning curve was much higher (1.25%) efficiency.

The FEL lased better with a non-design buncher gradient, about 10% higher than the one that produces the smallest energy spread at injection. PARMELA shows that the injected bunch is around 20% longer (which is good for alleviating longitudinal space charge forces), but the energy spread is about 30% larger. The optimal injector configuration for the FEL seems to be a compromise between the bunch length and energy spread at injection.

CONCLUSIONS

Extending the injector PARMELA model through the first cryo-module confirmed observations of an asymmetry in the final energy spread of the electron beam after acceleration and a significant growth in the longitudinal emittance. The asymmetry can be explained by the interaction between the electric field within the electron bunch created by space charge forces, and the electric field from the RF system during acceleration. Injecting a long bunch alleviates the longitudinal space charge force. PARMELA modeling provided guidance towards achieving a longer bunch at injection, simply operate the downstream cavity of the injector closer to crest. Once this was implemented in the machine, the asymmetry in the final beam energy spread was reduced, the longitudinal match throughout the accelerator became very close to lattice design, and the growth in the longitudinal emittance was decreased.

The interaction of the longitudinal space force with the RF system will be an important factor to consider in the design of high charge accelerators for FELs. Since the FEL gain depends on peak charge, it is desirable to have a short bunch with high charge at the wiggler. The present study reveals that bunch length at the wiggler is limited by the intrinsic longitudinal emittance of the beam generated during its creation, since the imposed phase/energy correlation in the energy spread by the RF system is removed by proper longitudinal phase space management, and the correlated (space charge) energy spread can be reduced by means of a long injected bunch.

ACKNOWLEDGMENTS

This work supported by The Office of Naval Research, the Joint Technology Office, NAVSEA PMS-405, the Air Force Research Laboratory, U.S. Army Night Vision Lab, the Commonwealth of Virginia, and by DOE Contract DE- AC05-84ER40150.

REFERENCES

1 Parmela_fel0.2: FEL Injector Simulation, JLAB-TN-03-028, K. B. Beard, B. Yunn, C. Hernandez-Garcia

2 D. Douglas et al., "Driver accelerator design for the 10 kW Upgrade for the Jefferson Lab IR FEL", LINAC2001, pp. 867-9, Monterey, CA 2001.

3 D. Engwall, et al., PAC'97, pp. 2693-5, Vancouver, May 1997.

4 C. Hernandez-Garcia, these proceedings.

5 T. Siggins et al., "Performance of a GaAs DC photocathode gun for the Jefferson Lab FEL", *Nucl. Inst. Meth.* A 475 (2001) 549-553.

6 B. C. Yunn, "Physics of the JLab FEL injector", PAC'99, pp. 2453-5, New York, April 1999.

7 J. R. Delayen et al., PAC'99, pp. 934-6, New York, 29 March-2 August 1999.

8 J. Flanz et al., *Nucl. Inst. Meth.* A421:325 –33 (1985).

9 WesCam©, developed by W. Moore, JLab FEL.

10 D. Douglas, private communication.